Developmental Biology **244,** 342–357 (2002)
doi:10.1006/dbio.2002.0602, available online at http://www.idealibrary.com on IDEAL®



# Movements during Gastrulation through Wnt/$Ca^{2+}$ Signaling Pathway

**Sun-Cheol Choi and Jin-Kwan Han**[1]

*Division of Molecular and Life Sciences, Pohang University of Science and Technology, San 31 Hyoja Dong, Pohang, Kyungbuk, 790-784, Republic of Korea*

**Rho GTPases are molecular switches that regulate many essential cellular processes, including actin dynamics, cell adhesion, cell-cycle progression, and transcription. We have isolated the *Xenopus* homolog of Rho GTPase Cdc42 and examined its potential role during gastrulation movements in early *Xenopus* embryos. XCdc42 is expressed in tissues undergoing extensive morphogenetic changes, such as the deep layers of involuting mesoderm and posterior neuroectoderm during gastrulation, and somitic mesoderm at neurula stages. Overexpression of either wild-type (WT) or dominant-negative (DN) XCdc42 interferes with convergent extension movements in intact embryos, activin-stimulated animal caps, and dorsal marginal zone explants. These effects occur without affecting mesodermal specification. Overexpression of WT or DN XCdc42 leads to the decrease and increase of cell adhesiveness of blastomeres, respectively, as demonstrated by the cell adhesion assay. In addition, when overexpressed, PKC-$\alpha$, XWnt-5a, and Mfz-3 inhibit activin-induced convergent extension in animal cap explants. This inhibition can be rescued by coexpression of DN XCdc42, implying that XCdc42 acts downstream of the Wnt/$Ca^{2+}$ signaling pathway involving PKC activation. XCdc42 also lies downstream of XWnt-5a in the regulation of $Ca^{2+}$-dependent cell adhesion. Taken together, our results suggest that XCdc42 plays a role in the regulation of convergent extension movements during gastrulation through the protein kinase C-mediated Wnt/$Ca^{2+}$ pathway.** 

***Key Words: Xenopus*; Wnt/$Ca^{2+}$ pathway; Cdc42; cell adhesion; gastrulation; XWnt-5a; Mfz-3; PKC.**

## INTRODUCTION

The morphogenetic movements of gastrulation are critical for establishing the three germ layers—ectoderm, mesoderm, and endoderm—and embryonic axis. In *Xenopus* embryos, these cell movements involve both involution and convergent extension. During convergent extension movement, polarized dorsal mesodermal cells intercalate in a mediolateral direction to produce a pronounced elongation of the anterior–posterior axis (Keller, 1991; Keller *et al.*, 1992). The molecular mechanisms by which mesodermal cells become polarized and convergent extension is driven, however, remain poorly understood.

Recent evidence has suggested a role of a Wnt signaling pathway in the regulation of cell behavior during gastrulation (Wallingford *et al.*, 2000; Tada and Smith, 2000; Djiane *et al.*, 2000; Heisenberg *et al.*, 2000). Wnts are a family of secreted glycoproteins that are involved in a variety of developmental processes, such as cell migration, cell proliferation, and cell polarity (Dale, 1998). Based on functional assays in *Xenopus* embryos and mammalian cell lines, vertebrate Wnts have been grouped into two functional classes (Miller *et al.*, 1999; Kühl *et al.*, 2000a). Ectopic expression of the first group, called Wnt-1 class (Wnt-1, Wnt-8, Wnt-8b, and Wnt-3a), induces a secondary axis in the early *Xenopus* embryo (Du *et al.*, 1995) and transforms the epithelial cell line (Wong *et al.*, 1994). This transforming class of Wnt ligands activates the canonical Wnt/$\beta$-catenin signaling pathway that involves the stabilization of $\beta$-catenin (Moon and Kimelman, 1998). $\beta$-Catenin then activates, in the nucleus, the expression of specific target genes such as siamois and Xnr3 in *Xenopus* embryos (Smith *et al.*, 1995; Lemaire *et al.*, 1995). On the other hand, members of the Wnt-5a class (Wnt-4, Wnt-5a, and Wnt-11) are not axis-inducing in *Xenopus* embryos nor do they

[1] To whom correspondence should be addressed. Fax: 82-54-279-2199. E-mail: jkh@postech.ac.kr.



0012-1606/02 $35.00

transform mammalian cell line. This class of Wnts can also antagonize the activities of Wnt-1 class signaling and they decrease cell adhesion (Torres *et al.*, 1996). Members of the Wnt-5a class trigger a signaling cascade, referred to as the Wnt/$Ca^{2+}$ pathway, that is thought to stimulate intracellular calcium release in a G-protein-dependent manner and then activate protein kinase C (PKC) (Slusarski *et al.*, 1997a,b; Sheldahl *et al.*, 1999) and $Ca^{2+}$/calmodulin-dependent kinase II (CamKII) (Kühl *et al.*, 2000b). In addition, Wnt-11 has been shown to regulate convergent extension movements via Dishevelled (Dsh), resembling the planar cell polarity (PCP) pathway in *Drosophila*, in which Frizzled, a transmembrane receptor for Wnt ligands, and Dsh signal via small GTPase and Jun N-terminal kinase (JNK) to regulate cell shape and cell polarity (Tada and Smith, 2000; Wallingford *et al.*, 2000; Heisenberg *et al.*, 2000; Boutros *et al.*, 1998). However, little is known about the relationship between the PCP and Wnt/$Ca^{2+}$ pathways.

Rho GTPases have been implicated in a variety of cellular functions, including cytokinesis, cytoskeletal reorganization, cell adhesion, endocytosis, and cell cycle progression (Bishop and Hall, 2000; Schmitz *et al.*, 2000). Rho family proteins, which include Rho, Rac, and Cdc42, cycle between active, GTP-bound and inactive, GDP-bound forms. The Rho GTPases mediate a signaling pathway for the cell shape changes associated with morphogenetic movements in *Drosophila* gastrulation (Barrett *et al.*, 1997). In *Xenopus*, a dominant-negative (DN) mutant of human Cdc42 rescued the inhibitory effect of *Xenopus* frizzled 7 (Xfz7) on convergent extension in activin-treated animal cap explants, suggesting that Xfz7 signaling regulates cytoskeletal reorganization through Rho GTPase Cdc42 during convergent extension movement (Djiane *et al.*, 2000). However, it is not yet certain whether Cdc42 functions downstream of Dsh in morphogenetic movements. In a *Drosophila* planar polarity signaling pathway, Dsh activates JNK through the RhoA small GTPase (Strutt *et al.*, 1997). Genetic analysis in *Drosophila* showed that *Drosophila* Cdc42 does not function downstream of Dsh in planar polarity signaling (Boutros *et al.*, 1998). In addition, the DN of Cdc42 and Rac1 could not inhibit Dvl (mammalian Dsh homologue)-induced JNK activation, implying that Dvl may activate JNK via a novel pathway that does not involve Cdc42 and Rac1 (Lin *et al.*, 1999). Interestingly, Moriguchi *et al.* (1999) have shown that in the NIH-3T3 cell line, the same DN Cdc42 mutant inhibited Dsh-induced JNK activation. Taken together, it is possible that the functions of the Rho GTPases are slightly different from vertebrate to invertebrate and cell line to cell line.

To better understand the role of the Rho GTPases in the regulation of morphogenetic cell movements during *Xenopus* gastrulation, we have cloned a *Xenopus* Cdc42 homologue, XCdc42, and here report functional analysis of XCdc42 during gastrulation cell movement. *In situ* hybridization reveals that, while at gastrula stages, XCdc42 is expressed in the ectoderm and marginal zone, it can also be found in the deep layers of involuting mesoderm and posterior neuroectoderm that undergo extensive morphogenetic movements. Overexpression of either wild-type (WT) or DN XCdc42 in intact *Xenopus* embryos, activin-stimulated animal cap explants, and dorsal marginal zone (DMZ) explants impairs convergent extension movements without affecting mesodermal differentiation. Rescue analysis with different Dsh mutants and PKC demonstrates that XCdc42 functions independently of Dsh, but downstream of the Wnt/$Ca^{2+}$ signaling pathway involving PKC activation. Furthermore, we show that XCdc42 affects $Ca^{2+}$-dependent cell adhesion in embryonic cells. Finally, we provide evidence that XCdc42 lies downstream of XWnt-5a in the regulation of $Ca^{2+}$-dependent cell adhesion.

## MATERIALS AND METHODS

### *Eggs and Embryos*

Eggs were obtained from *Xenopus laevis* primed with 800 units of human chorionic gonadotropin (Sigma). They were *in vitro* fertilized by using macerated testis, dejellied in 2% cysteine solution (pH 7.8), and cultured in 0.33× Modified Ringer (MR) (Godsave *et al.*, 1988) until stage 8 and then transferred to 0.1× MR. Developmental stages of embryos were determined according to Nieuwkoop and Faber (1967).

### *Isolation of Xenopus Cdc42*

Degenerate primers directed at the highly conserved region among human, fly, and yeast Cdc42 clones were used in the amplification in the polymerase chain reaction (PCR) from stage 12 embryo cDNA. To obtain XCdc42 full-length cDNA, a PCR-generated fragment (269 bp) was used to screen a *Xenopus* stage 10 cDNA library constructed in the Lambda ZAPII bacteriophage vector (gift from Dr. Michael W. King). The complete nucleotide sequence of the clone containing the full-length XCdc42 has been deposited in GenBank under Accession No. AF247679.

### *Plasmid Constructs*

The entire coding region of XCdc42 was amplified by using the primer combinations 5′-CGGGATCCCGATGCAGACAATTAA-ATGT-3′ and 5′-GGAATTCCTCATAGCAGCATACACTT-3′ and cloned into the *Bam*HI and *Eco*RI sites of the pCS2+ vector. The constitutively active Cdc42 construct ($Cdc42^{G12V}$) and its DN mutant ($Cdc42^{T17N}$) have been described previously (Drechsel *et al.*, 1996). To obtain the DN version of XCdc42 ($XCdc42^{T17N}$), the single amino acid change from T to N at position 17 was achieved by generating two PCR products containing the point mutation from the full-length XCdc42 in the pBS-KS(+) vector. For the first PCR, the T7 primer and the 5′-GATAAGGAGACAGTTTTTACCCACAGC-3′ primer were used. In the second PCR, the T3 primer and the 5′-GCTG-TGGGTAAAAACTGTCTCCTTATC-3′ primer were used. These gel-purified PCR products containing an overlapping region were used in a third PCR, with T3 and T7 primers. The *Eco*RI fragment of this PCR product was used to replace the *Eco*RI fragment in the WT construct. For the constitutively active mutant of XCdc42 ($XCdc42^{G12V}$), the PCR scheme described above was followed. The first PCR used the T7 primer and the 5′-TACCCACAGCAACA-TCACCAACG-3′ primer. For the second PCR, the T3 primer and the

5′-CGTTGGTGATGTTGCTGTGGGTA-3′ primer were used. These mutants of XCdc42 were subcloned into the *Bam*HI and *Eco*RI sites of the pCS2+ vector to generate the expression constructs. The human PKC-$\alpha$ (hPKC-$\alpha$) coding sequence was cloned into the *Eco*RI and *Xba*I sites of the pCS2+ vector. pSP64T-XWnt-5A, pCS2-Mfz3, pSP64R1-XDsh, pCS2-XDsh-ΔDEP, and pCS2-XDsh-ΔPDZ were provided by Dr. Randall Moon.

### *mRNA Synthesis, Microinjection, and Explant Assay*

Capped synthetic sense mRNAs were generated by using the Ambion mMessage mMachine kit and SP6 polymerase. The expression constructs pCS2-XCdc42, pCS2-XCdc42$^{T17N}$, pCS2-XCdc42$^{G12V}$, pCS2-hPKC-$\alpha$, pCS2-Mfz3, pCS2-XDsh-ΔDEP, and pCS2-XDsh-ΔPDZ were linearized with *Not*I, and pSP64T-XWnt-5A and pSP64R1-XDsh were digested with *Xba*I. Microinjections of embryos were carried out in 0.33× MR containing 4% Ficoll-400. Embryos were injected at the four-cell stage with 4.6 nl of a solution containing mRNA into either the DMZ or animal pole region. Animal caps and DMZ explants were excised at stages 8.5 and 10, respectively. Dissected explants were cultured in 1× MR containing 10 $\mu$g/ml of bovine serum albumin, 50 $\mu$g/ml of gentamycin, and 5 $\mu$g/ml of streptomycin. For standard *Xenopus* animal cap assay, recombinant activin A (kindly provided by Dr. Ashasima) was added at a concentration of 10 ng/ml. Animal caps and DMZ explants were cultured until stages 18 and 20, respectively, and scored for elongation.

### *In Situ Hybridization*

Whole-mount *in situ* hybridization was performed with digoxigenin (DIG)-labeled probes, as described by Harland (1991). *In situ* hybridization on tissue sections was also carried out by using a DIG-labeled RNA probe as described previously (Henry *et al.*, 1996). All sections are 14 $\mu$m thick. Hybridization was detected with an alkaline-phosphatase-coupled anti-DIG antibody and visualized by using BM purple as a substrate (Roche Molecular Biochemicals). An anti-sense *in situ* probe against XCdc42 was generated by linearizing the pBS-KS-XCdc42 construct with *Hin*dIII and transcribing with the T3 RNA polymerase. XCdc42 sense probe was synthesized by using the T7 RNA polymerase on *Bam*HI-linearized template. No positive staining was seen in the sense control. The template constructs for *in situ* probe against chordin, XmyoD, and Xnot were obtained by PCR. Xbra (Smith *et al.*, 1991) and Otx-2 (Lamb *et al.*, 1993) are as previously reported.

### *RT-PCR*

Total RNA was prepared from embryos or animal cap explants with TRI reagent (Sigma) and treated with RNase-free DNase I (Roche Molecular Biochemicals) to remove genomic DNAs. RNA was transcribed by using M-MLV reverse transcriptase (Promega) at 37°C for 1 h. PCR amplification was performed by using *Taq* polymerase (TaKaRa) as described by Kim and Han (1999). PCR products were analyzed on 2% agarose gels with ethidium bromide, and fluorescent DNA fragments were digitized and quantitated by using a fluorescent image analyzer FLA-2000 (Fuji Film, Tokyo). Primers for XCdc42 were: (forward) 5′-TCTTAGCTATCCACAGACAGACGTGTT-3′ and (reverse) 5′-TCATAGCAGCATACACTTGCGTTT-3′ (370 bp, 25 cycles). Primers for Xbra (Gawantka *et al.*, 1995), chordin, ODC (Bouwmeester *et al.*, 1996), EF-1$\alpha$ (Kengaku and Okamoto, 1995), gsc (Lemaire and Gurdon, 1994), and muscle actin (http://vize222.zo.utexas.edu/Marker pages/primers.html) were as previously described.

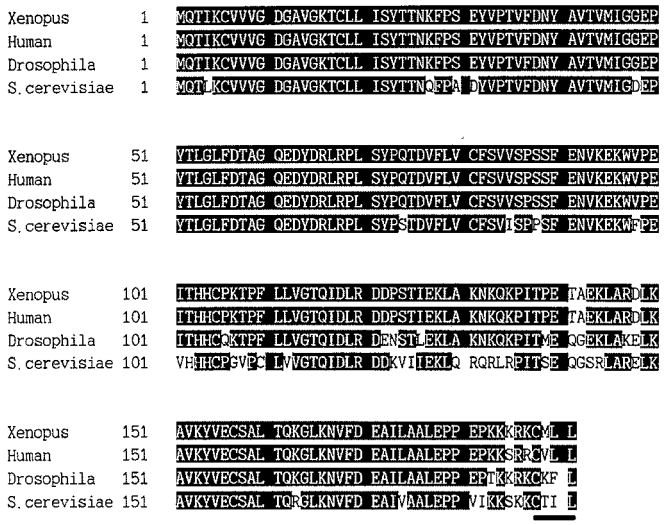


**FIG. 1.** Alignment of the deduced amino acid sequence of *Xenopus* Cdc42 with the human, *Drosophila*, and *S. cerevisiae* Cdc42 proteins. Identical residues are indicated by shading. The C-terminal CAAX-box, a site of lipid modification, is underlined.

### *Cell Adhesion Assay*

Cell adhesion assay was carried out as previously described (Torres *et al.*, 1996). Briefly, embryos were injected at the four-cell stage into the animal pole or DMZ region with WT and/or DN XCdc42 mRNA. Animal caps and DMZ explants were excised at stages 8 and 10, respectively, and dissociated to a single cell suspension in $Ca^{2+}$/$Mg^{2+}$-free Modified Barth's Solution (MBS) (88 mM NaCl, 1 mM KCl, 2.4 mM $NaHCO_3$, 10 mM Hepes, pH 7.4) for 2 h. Cells were subsequently reaggregated at room temperature in MBS with 4 mM $Ca^{2+}$ by horizontal rocking for 30–50 min and fixed by adding formaldehyde to 3.7%. Cell reaggregation was analyzed by photographing random cell populations from each treatment and scoring blind for cell clumping. Changes in cell adhesiveness were determined by analyzing the relative number of large and small cell clumps formed in the reaggregation assays relative to control experiments.

## RESULTS

### *Isolation and Expression Pattern of Xenopus Cdc42*

A PCR-based cloning strategy was used to obtain a *Xenopus* homolog of Cdc42, a member of Rho GTPase. The *Xenopus* Cdc42 cDNA we isolated, named XCdc42, encodes a 191-residue polypeptide. It contains a C-terminal CAAX-motif that serves as a prenylation site. Sequence comparison shows that *Xenopus* and human Cdc42 are quite similar with 98% amino acid identity (Fig. 1). XCdc42 is also 93 and 80% identical at the amino acid level to the *Drosophila* and *Saccharomyces cerevisiae* Cdc42, respectively. A temporal expression pattern analyzed by RT-PCR indicates that XCdc42 is expressed at relatively constant

levels throughout early embryogenesis (Fig. 2A). *In situ* hybridization was performed to examine the spatial expression pattern of XCdc42 in early development. In the fertilized egg, XCdc42 was found to be localized to the animal hemisphere, and this distribution pattern continued into blastula stage (data not shown). From the mid- to late-gastrula stages, its transcripts were expressed in the mesoderm and overlying ectoderm as the marginal zone cells migrate inward. Note that it is also present in the deep cells of involuting dorsal mesoderm and posterior neuroectoderm that are undergoing extensive cell polarization and rearrangements (Fig. 2B, a–d). Relatively strong expression of XCdc42 was detectable in the superficial layer of the DMZ, with lower levels of its message in the deep layers (Fig. 2B, d). At midneurula stage, the positive stainings were observed in the notochord, somitogenic mesoderm, and ectodermal cells (Fig. 2B, e). During the tailbud stage, XCdc42 messages were also found in the neural tube and pronephric anlage (Fig. 2B, f). Intriguingly, with the onset of tailbud stage, strong expressions of XCdc42 in the somitogenic mesoderm were barely detectable (Fig. 2B, e and f). Overall, the localization pattern of XCdc42 appears to be consistent with expression at sites of movement and rearrangement of cells in early development, particularly in the involuting marginal zone and somitogenic mesoderm.

### *XCdc42 Affects Cell Movements in Gastrulation*

To define the embryonic function of XCdc42, various levels of synthetic XCdc42 mRNA were injected into the marginal zone at the four-cell stage. Injection of either WT or DN XCdc42 mRNA (200 pg each) in the dorsal equatorial region led to two distinct features (Fig. 3; and Table 1). One is characterized by a severe dorsal flexure and a failure of neural folds to fuse, a phenotype that is produced by strong inhibition of neural convergent extension (Wallingford and Harland, 2001). The other includes shortened anteroposterior axis and stout morphology that are caused by strongly suppressing mesodermal convergent extension (Wallingford and Harland, 2001). These phenotypes were presaged at earlier stages by cell movement defects in gastrulation and failure of neural plate closure (data not shown).

To determine whether overexpression of XCdc42 directly affects cell behavior, we examined the expressions of chordin, Xbra, XMyoD, and Otx-2 mRNAs in XCdc42-injected embryos. Prior to the onset of convergent extension movements, the distributions of chordin and Xbra were identical in control uninjected and XCdc42-injected embryos (Fig. 4A, a and c), suggesting that XCdc42 overexpression had no obvious effect on mesoderm specification. In late gastrula stages, chordin was found in the lateral regions of the blastopore in a XCdc42-injected embryo, whereas in an uninjected control embryo, it was expressed in the prechordal plate and notochord (Fig. 4A, b). Expression of Xbra in stage 12 control embryos was detected around the blastopore and in the notochordal mesoderm (Fig. 4A, d). In XCdc42-injected embryos, the circumblastoporal localization of Xbra was wider and its expression in the notochordal mesoderm was absent or reduced compared with control embryos (Fig. 4A, d). With XmyoD being restricted to the lateral mesoderm in uninjected control embryos (Fig. 4A, e), it was expressed in both the lateral and ventral marginal zone in XCdc42-injected late gastrulae (Fig. 4A, f), clearly indicating that dorsal mesoderm failed to involute. At early neurula stage, an Otx-2-positive domain was localized in the dorsal ectoderm more posteriorly in XCdc42-injected embryos than in control embryos (Fig. 4A, g and h). *In situ* hybridization to XmyoD and Xnot in XCdc42-injected embryos at later stages showed that differentiation of muscle and notochord was not affected by XCdc42, although these embryos exhibited incomplete neural plate closure and shortened axis (Fig. 4B). These results suggest that XCdc42 overexpression inhibits movements of mesodermal cells without affecting the expressions of mesodermal and neural markers.

### *XCdc42 Interferes with Convergent Extension Movements*

To test further the effect of XCdc42 on cell movements, an animal cap assay was performed in which convergence and extension movements are induced by treating animal cap explants with activin (Symes and Smith, 1987). In animal cap explants from uninjected embryos, addition of

**FIG. 2.** Expression pattern of XCdc42 in early development. (A) Temporal expression pattern of XCdc42. Developmental stages are shown above each lane. Ornithine decarboxylase (ODC) was used as a loading control. (B) Spatial expression pattern of XCdc42. (a) Sagittal section of a stage 11 gastrula. An arrow indicates dorsal lip of blastopore. (b) Higher magnified view of (a). XCdc42 transcripts are detectable in the deep cells of involuting mesoderm (arrowheads) and in the presumptive neuroectoderm (arrows). (c) Sagittal section of a stage 12 gastrula. Arrowheads indicate involuting mesoderm. (d) Higher magnified view of (c). Relatively low levels of XCdc42 expression are present in the deep layers of dorsal mesoderm (arrowheads), with its strong expression in the overlying ectoderm (arrows). (e) Transverse section of an early neurula. Strong expression of XCdc42 is present in the neural plate (NP), somitic mesoderm (S), notochord (No), and ectoderm. (f) Cross section of a tailbud stage embryo. XCdc42 is expressed in the pronephric anlage (PA), neural tube, and notochord, but not in the segmented somites (S).

**FIG. 3.** Gain and loss of XCdc42 function have similar effects on the gastrulation movement. Embryos were injected into the DMZ at the four-cell stage with 200 pg of either WT or DN XCdc42 mRNA and allowed to develop to stage 32. Prolactin-injected control embryos (A) were normal, whereas embryos expressing WT XCdc42 (B) or DN XCdc42 (C) displayed similarly two distinct phenotypes; one is dorsally kinked and has an open neural tube. The other is stout and fails to straighten the A/P axis. Lateral view is shown; anterior is to the left.

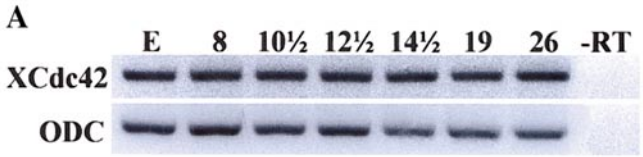


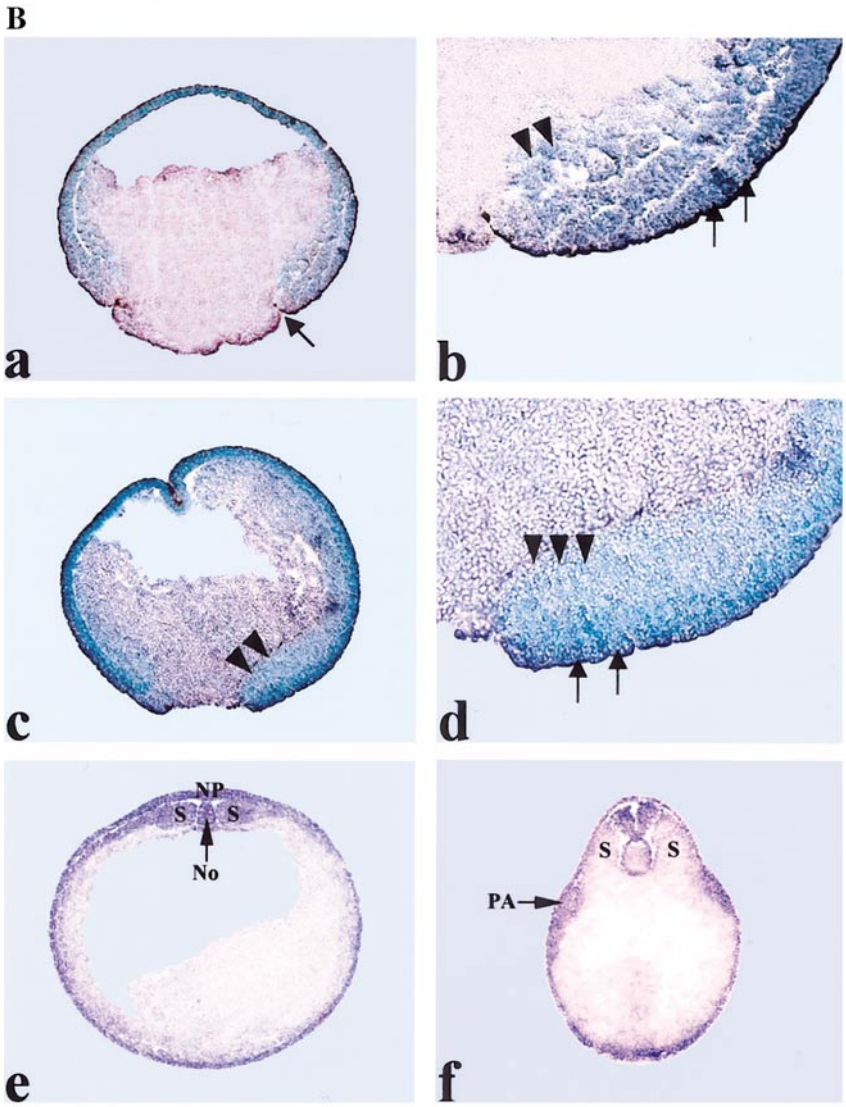


2

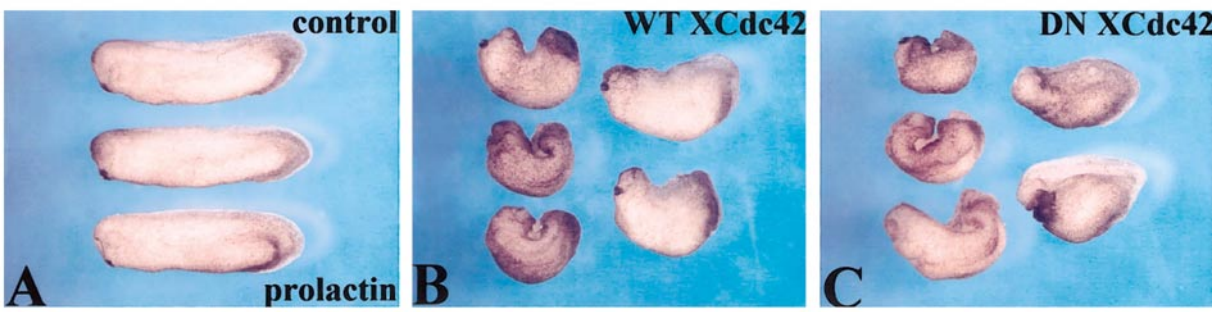


3

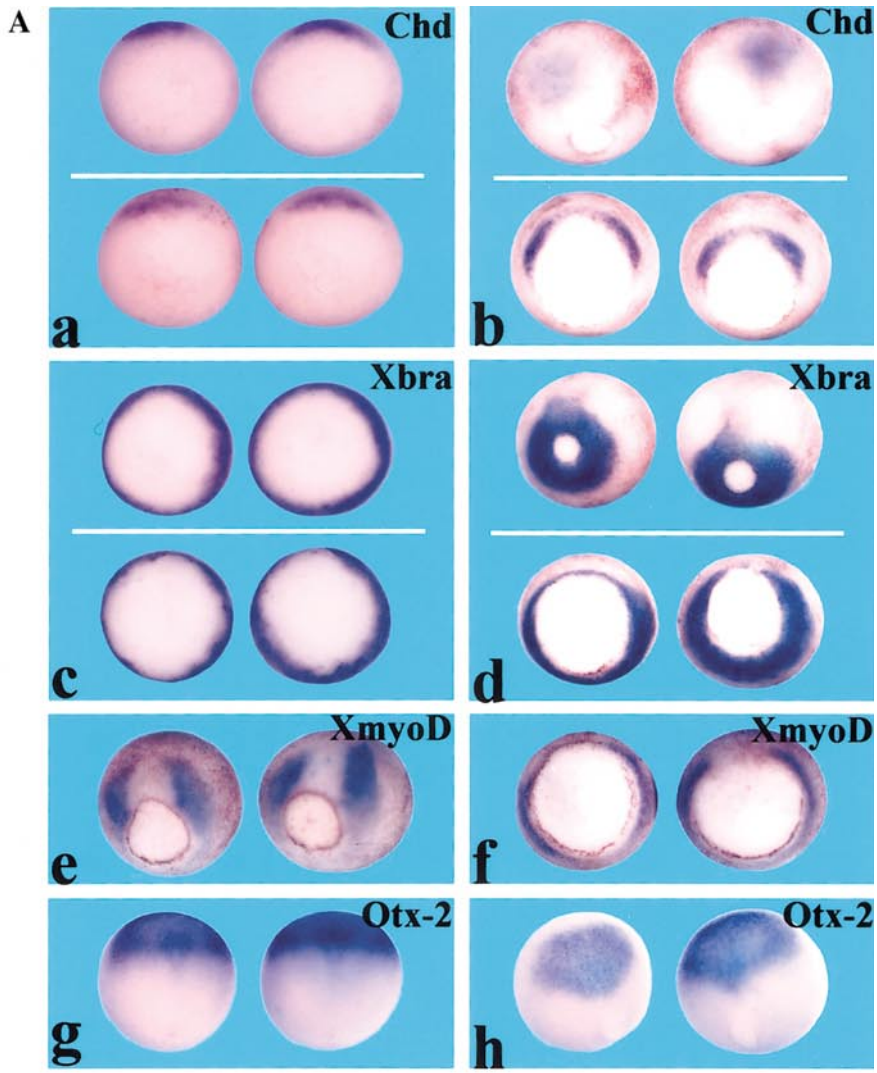


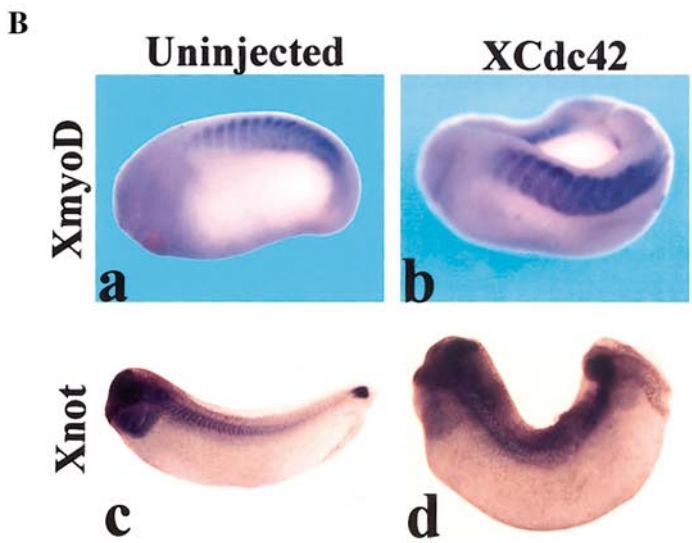

**TABLE 1**
*XCdc42* Affects Gastrulation Movement

| RNA injected (pg) | *n* | Blastopore | | Late phenotypes | | |
|---|---|---|---|---|---|---|
| | | Normal | Open | Normal | Truncated | Bent axis |
| Prolactin (200) | 66 | 85 | 15 | 82 | 8 | 10 |
| WT XCdc42 (200) | 65 | 12 | 88 | 9 | 75 | 16 |
| CA XCdc42 (25) | 52 | 6 | 94 | 2 | 54 | 44 |
| DN XCdc42 (200) | 66 | 21 | 79 | 20 | 61 | 19 |

*Note.* Embryos were injected at the four-cell stage into the DMZ. Blastopore closure and axis phenotypes were scored at stage 14 and 35, respectively. Numbers refer to percentages of phenotypes: *n*, total numbers of embryos scored.

activin caused extensive elongation (Fig. 5A, a), but injection of either WT or DN XCdc42 inhibited this elongation significantly (Figs. 5A, b and c, and 5C). Coinjection of DN XCdc42 efficiently reversed the inhibition caused by WT XCdc42, suggesting the specific effect of XCdc42 on activin-induced convergent extension (Figs. 5A, d and 5C). This inhibition of animal cap elongation by changes in XCdc42 expression occurred without affecting the mesodermal differentiation, which was determined by RT-PCR analysis of the expressions of the dorsal mesodermal markers goosecoid, chordin, the panmesodermal marker Xbra, and muscle actin (Fig. 5D). Taken together, these results suggest that certain levels of XCdc42 activity are required for convergent extension movements in explants, but not for mesodermal differentiation.

We further examined the inhibitory effects of XCdc42 on DMZ tissue, which undergoes convergent extension in intact embryos. In contrast to the extensive elongation of uninjected control explants, this process was largely inhibited in either WT or DN XCdc42-injected explants (Figs. 5B and 5C). As with animal cap explants, some DMZ tissues exhibited weak morphogenetic movements; however, the difference in mean elongation between XCdc42-injected and control explants was highly significant (Fig. 5C).

### *XCdc42 May Function Downstream of the Wnt/$Ca^{2+}$ Pathway Involving PKC Activation*

Recently, it has been shown that Dsh is involved in the morphogenetic movement by controlling cell polarity during gastrulation (Wallingford *et al.*, 2000) and its activity is regulated by Wnt-11 during convergent extension (Heisenberg *et al.*, 2000; Tada and Smith, 2000). To examine the possibility that XCdc42 might be implicated in Dsh-mediated morphogenetic process, we examined whether either a DN or a constitutively active (CA) XCdc42 mutant could rescue the effects of WT and PDZ or DEP domain-deleted Dsh on the elongation of activin-treated animal caps and vice versa. However, neither XCdc42 mutant could reverse the inhibition of explant elongation caused by overexpression of these Dsh constructs and vice versa (data not shown), suggesting that XCdc42 functions independently of Dsh in convergent extension movements.

We next investigated whether XCdc42 may participate in PKC activation involving the Wnt/$Ca^{2+}$ signaling pathway. XWnt-5a and mouse frizzled 3 (Mfz-3) have been implicated in triggering a signaling cascade that involves G-protein activity, intracellular $Ca^{2+}$ release, and PKC activation (Kühl *et al.*, 2000a). Overexpression of human PKC-$\alpha$

**FIG. 4.** XCdc42 overexpression affects the localization of mesodermal and neural markers. Four-cell stage embryos were injected in the DMZ with 200 pg of WT XCdc42 mRNA. (A) (a) Expression of chordin at stage 10 in uninjected control (upper) and XCdc42-injected (lower) embryos (vegetal view is shown; dorsal at top). (b) Expression of chordin in uninjected (upper, dorsovegetal view; anterior at top) and XCdc42-injected (lower, vegetal view; dorsal at top) embryos at stage 12. In XCdc42-injected embryos, chordin-expressing cells did not converge toward the dorsal midline and were still localized around the blastopore. (c) The pattern of Xbra expression in uninjected (upper) and XCdc42-injected (lower) embryos at stage 10 (vegetal view; dorsal at top). (d) Expression of Xbra in stage 12 control (upper, dorsovegetal view) and XCdc42-injected (lower, vegetal view; dorsal at top) embryos. Xbra transcripts, which were detectable in the notochordal mesoderm in uninjected control embryos, were absent in XCdc42-injected embryos, indicating the failure of dorsal mesoderm to involute during gastrulation. (e, f) The expression of XmyoD in uninjected (dorsovegetal view) and XCdc42-injected (vegetal view; dorsal at top) embryos at stage 11.5, respectively. In XCdc42-injected embryos, XmyoD remained expressed around the blastopore, but not in the lateral mesoderm. (g) At stage 13, uninjected control embryos had the anterior expression of Otx-2 (dorsal view is shown; anterior at top). (h) In XCdc42-injected embryos at stage 13, the expression of Otx-2 occurred in the dorsal ectoderm (dorsovegetal). (B) (a, b) *In situ* hybridization against XmyoD was performed on both uninjected (a) and XCdc42-injected (b) embryos at stage 25. XCdc42-injected embryos failed to close the neural plate, yet retained muscle differentiation. (c, d) As in the uninjected embryo at stage 30 (c), notochord differentiation normally occurred in the XCdc42-injected embryo (d) as assessed by expression of Xnot.

mRNA resulted in the inhibition of elongation in animal cap explants stimulated with activin (Figs. 6A, b and 6C). Intriguingly, coinjection of DN XCdc42 efficiently rescued the inhibitory effect of human PKC-$\alpha$ on activin-induced convergent extension (Figs. 6A, c and 6C), implying that XCdc42 acts downstream of PKC-$\alpha$ in the morphogenetic process. While control uninjected explants extensively elongate in response to activin (Figs. 6B, a and 6C), explants from embryos injected with either XWnt-5a or Mfz-3 mRNA showed the inhibited elongation (Figs. 6B, b and d, and 6C). However, coexpression of DN XCdc42 with these mRNAs efficiently recovered explant elongation (Figs. 6B, c and e, and 6C).

Overall, the data above indicate that XCdc42 may be an effector of PKC-mediated Wnt/$Ca^{2+}$ signaling pathway in convergent extension movements.

### *XCdc42 Affects the Adhesive Properties of Embryonic Cells*

XCdc42 has been shown to regulate the cadherin-mediated cell–cell adhesion (reviewed in Kaibuchi *et al.*, 1999). To test whether XCdc42 might affect convergent extension by changing the adhesive properties of embryonic cells, a blastomere aggregation assay using DMZ and animal cap cells was carried out in which explants from embryos injected with either WT and/or DN XCdc42 mRNA were dissociated in $Ca^{2+}$/$Mg^{2+}$-free medium, and subsequently were reaggregated by adding $Ca^{2+}$-containing solution. In this assay, cell adhesion was defined as the ability of dissociated cells to reaggregate in the presence of $Ca^{2+}$. Explant cells from embryos coinjected with green fluorescent protein (GFP) mRNA as a lineage tracer and a test mRNA were fluorescent (data not shown), indicating that most cells which were scored for cell adhesion either expressed protein from the injected RNAs or were in contact with such cells. Cells from uninjected explants often reaggregated into large clumps in a $Ca^{2+}$-dependent manner (Figs. 7B, 7E, and 7F). However, overexpression of WT XCdc42 mRNA decreased the $Ca^{2+}$-dependent cell adhesion in both DMZ and animal cap cells, leading to the vast majority of cells remaining isolated from each other after $Ca^{2+}$ addition (Fig. 7C), and most clumps from these cells were in the small size range (Figs. 7E and 7F), implying the reduced adhesiveness to each other in WT XCdc42-injected cells. Injection of DN XCdc42 mRNA resulted in a little higher percentage of large clumps than dissociated control explants in cell adhesion assay (Figs. 7E and 7F). Interestingly, injection of DN XCdc42 caused embryonic tissue to be sometimes thicker than control tissue as revealed by microscopic observation (data not shown). The effects of overexpression of DN XCdc42 mRNA could also be observed during the dissociation procedure. Cells injected with DN XCdc42 became much more tightly associated and could not be easily dissociated in $Ca^{2+}$/$Mg^{2+}$-free solution. WT XCdc42-injected cells, however, were readily dissociated. In addition, the effect of WT XCdc42 to decrease $Ca^{2+}$-dependent cell adhesion could be rescued to a degree of adhesiveness resembling that of untreated control cells by coexpressing DN XCdc42 mRNA (Figs. 7D, 7E, and 7F). Taken together, these results suggest that certain levels of XCdc42 activity are required for a fine balance of $Ca^{2+}$-dependent cell adhesion in embryonic cells, which is important for convergent extension movements in DMZ and activin-stimulated animal cap explants (Huttenlocher *et al.*, 1995; Brieher and Gumbiner, 1994).

### *XCdc42 Lies Downstream of XWnt-5a in the Control of $Ca^{2+}$-Dependent Cell Adhesion*

As demonstrated above, XCdc42 functions downstream of the XWnt-5a-triggered signaling pathway in convergent extension. In addition, overexpression of XWnt-5a mRNA inhibits morphogenetic movements by decreasing cell adhesion (Torres *et al.*, 1996). So, we next examined whether XCdc42 could rescue the effect of XWnt-5a overexpression on $Ca^{2+}$-dependent cell adhesion. Cells expressing XWnt-5a mRNA did not reaggregate as efficiently as control uninjected cells, forming clumps of 20 or more cells in only 9% of clumps (Figs. 8B and 8D). The effect of XWnt-5a, however, could be overcome by coinjection of DN XCdc42 and XWnt-5a mRNA, resulting in clumps of more than 20 cells

**FIG. 5.** XCdc42 affects convergent extension, but not mesoderm induction. (A) Embryos were injected as indicated into the animal pole of four blastomeres at the four-cell stage. Animal cap explants were excised at stage 8.5, treated with 10 ng/ml recombinant activin, and cultured to the equivalent of stage 18. (a) Animal cap explants from uninjected control embryos elongated significantly in response to activin. (b) WT XCdc42 mRNA (400 pg) injection interfered with activin-induced explant elongation. (c) Animal cap explants injected with DN XCdc42 mRNA (2 ng) failed to elongate. (d) Coinjection of WT XCdc42 mRNA (400 pg) together with DN XCdc42 mRNA (400 pg) rescued the elongation of animal caps. (B) Injections were targeted to the DMZ at the four-cell stage. DMZ explants were excised at stage 10 and cultured to stage 20 before being measured for elongation. (a) Uninjected control DMZ explants elongated significantly. Injection of either (b) WT XCdc42 (400 pg) or (c) DN XCdc42 (2 ng) suppressed convergent extension of DMZ explants. (C) Quantitation of convergent extension of animal cap (AC) and DMZ explants. RNAs expressed are shown below graph. n, total number of explants. (D) RT-PCR analysis detecting expression of mesodermal markers in animal caps derived from embryos injected with XCdc42 constructs. Animal caps from embryos injected with either WT XCdc42 (400 pg) alone or WT and DN XCdc42 (400 pg each) were treated with activin at stage 8.5 and cultured until stage 10.5 for analysis of goosecoid (gsc), Xbra, and chordin (Chd) expression and until stage 23 for analysis of muscle actin (M. actin) expression. ODC and EF-1$\alpha$ are loading controls.

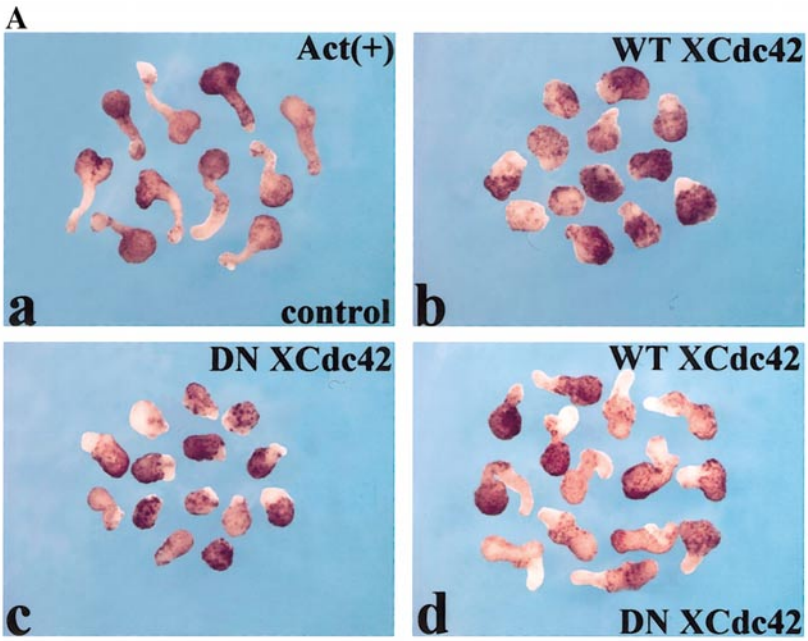


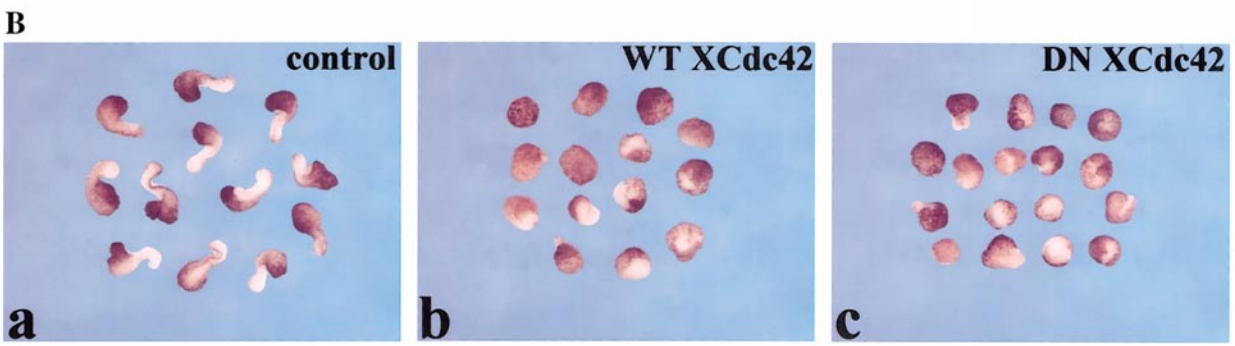


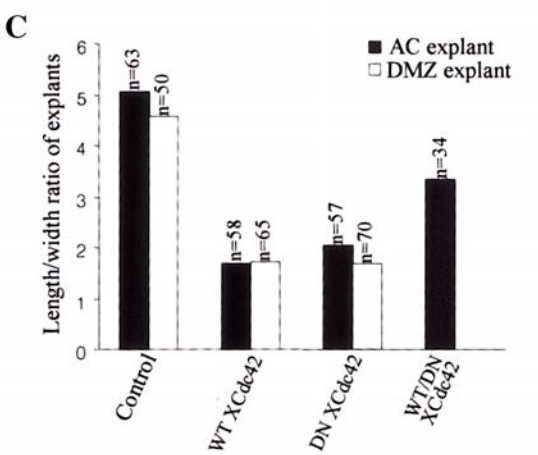


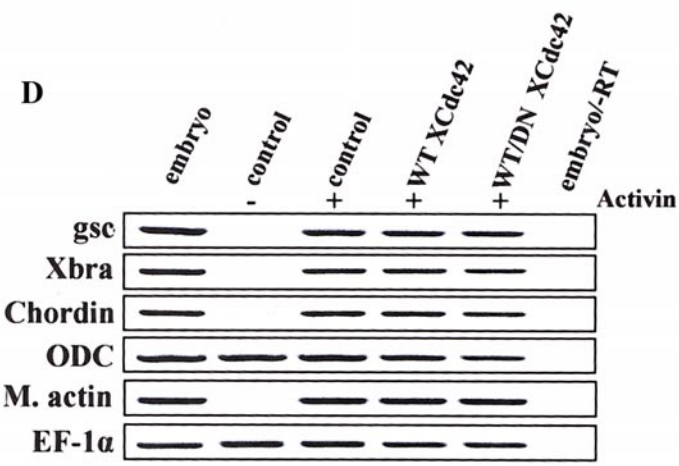

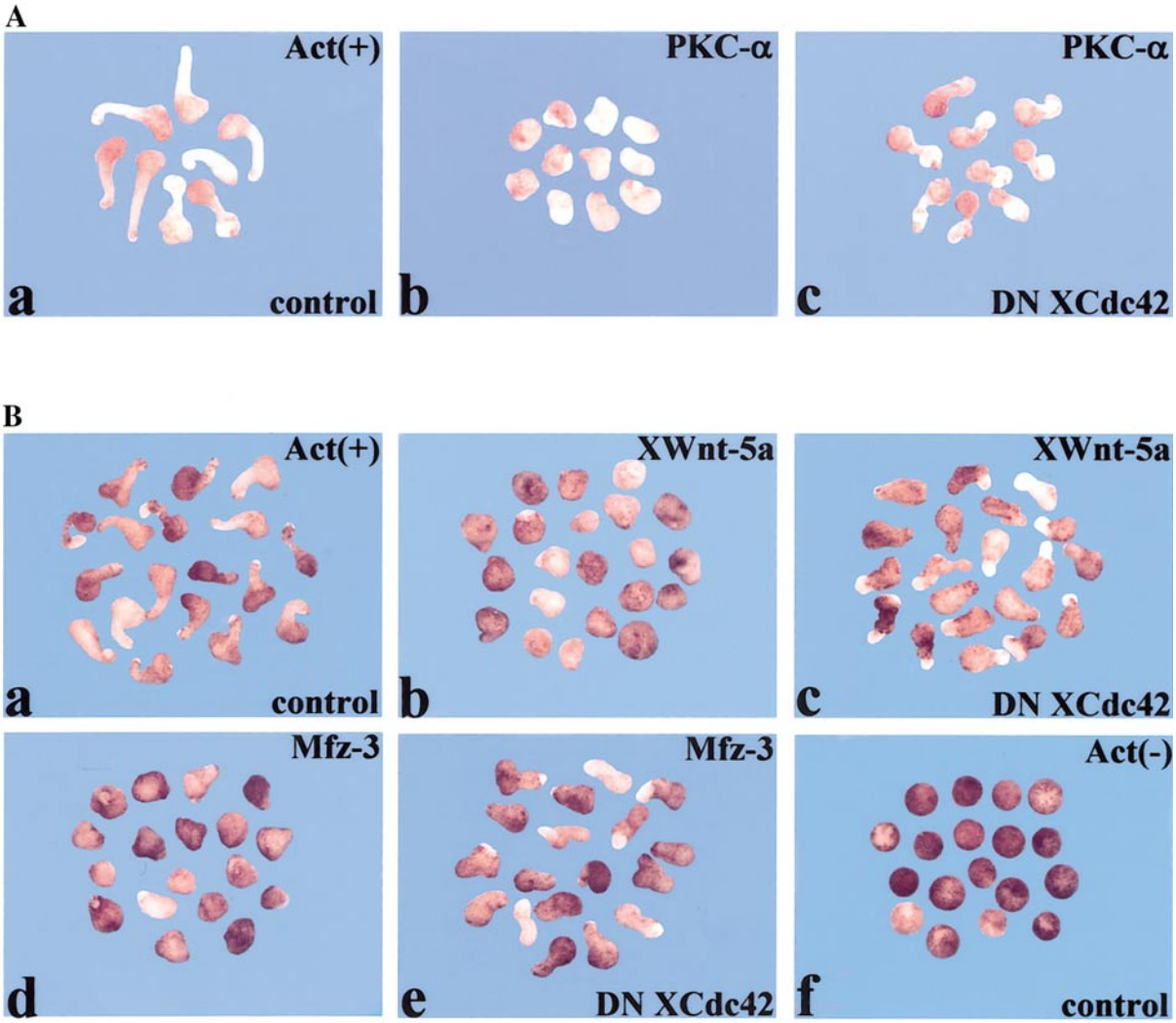


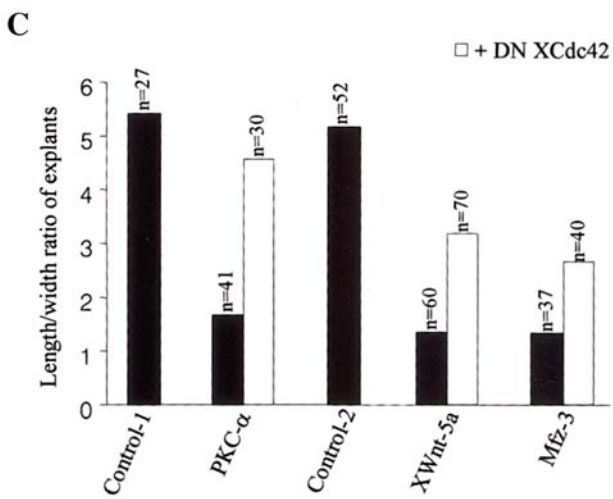

being formed in 42% of clumps (Figs. 8C and 8D). Together, these data suggest that XCdc42 may act downstream of XWnt-5a in the control of $Ca^{2+}$-dependent cell adhesion.

## DISCUSSION

In *Xenopus*, convergent extension movements involve changes in cell polarity, cell adhesion, and cell shape. The Rho GTPases have been implicated in a wide variety of cellular processes, including cytoskeletal organization, cell adhesion to the substratum, and cell polarity (Schmitz *et al.*, 2000; Erickson and Cerione, 2001). In this respect, they are likely to be good candidates for regulators of convergent extension movements.

In this study, we provide evidence that *Xenopus* Cdc42 may participate in the regulation of convergent extension movements during gastrulation. First, at gastrula stages, XCdc42 is present in the ectoderm and mesoderm, while it is also expressed in the deep layers of involuting dorsal mesoderm and posterior neuroectoderm in which cells become polarized and are extensively rearranged. XCdc42 messages are detectable in unsegmented somitic mesoderm during the neurula stage, after which they are no longer expressed in segmented somite areas (Fig. 2B). This expression pattern in the somite region has similarity to those of XRnd1 and Xfz7 molecules, which are also expressed only in unsegmented somitic mesoderm undergoing active morphogenetic processes (Wünnenberg-Stapleton *et al.*, 1999; Djiane *et al.*, 2000). Together, the overall expression pattern of XCdc42 suggests its role in the control of morphogenetic events in early *Xenopus* embryos.

Secondly, overexpression of either WT or DN XCdc42 in the dorsal equatorial region of *Xenopus* embryo inhibits convergent extension and delays mesoderm involution. The two phenotypes generated by injection of XCdc42 at the four-cell stage (Fig. 3) are similar to the ones produced by targeted injection of Dsh, XWnt-5a, or Nxfz-8 into dorsal animal or dorsal vegetal regions at the eight-cell stage (Wallingford and Harland, 2001); this result seems likely to derive from subtly different injection sites in DMZ, biasing injections vegetally or animally. However, all these characteristics are consequences of the failure of neural and mesodermal convergent extension. Consistent with these phenotypes, XCdc42 is expressed in the involuting dorsal mesoderm and in the posterior neural ectoderm, which undergo extensive convergent extension (Fig. 2). In addition, XCdc42 affects the elongations of activin-stimulated animal caps and DMZ explants (Fig. 5), which lengthen *in vitro* as a result of convergent extension, mimicking morphogenetic cell behavior during gastrulation in intact embryos. Together, these results implicate XCdc42 as a functional effector in the regulation of convergent extension movements.

Gain and loss of XCdc42 function both inhibit convergent extensions in intact embryos, activin-treated animal caps, and DMZ tissue explants. In *Drosophila* planar polarity signaling, overexpression of fz1, a putative Wnt receptor, results in tissue polarity phenotype resembling that of a loss-of-function mutation (Krasnow and Adler, 1994). WT *Xenopus* Wnt-11 also behaves like DN Wnt-11 in that both inhibit convergent extension movements in whole embryos and activin-treated explants (Tada and Smith, 2000). A reasonable explanation for the phenomenon that gain- and loss-of-function of a gene produce a similar phenotype may be found in a cell adhesion assay using XCdc42. In a gain-of-function situation, injection of WT XCdc42 inhibits $Ca^{2+}$-dependent cell reaggregation (Fig. 7C), whereas overexpression of DN XCdc42 makes stronger the adhesion between the neighboring cells (Figs. 7E and 7F), leading to the dissociation of explants being more difficult. These results suggest that excessive changes in XCdc42 activity disrupt the normal strength of adhesiveness between cells. Gastrulation movements are known to be maintained by a fine balance of temporally and spatially regulated cell adhesion (Huttenlocher *et al.*, 1995). In addition, activin-induced elongation of animal cap explants is associated with a decrease in cadherin-mediated cell adhesion (Brieher and Gumbiner, 1994). That is, activin induction could lower the avidity of cadherin and decrease cell–cell adhesion to allow cell movements, implying that appropriate levels of adhesiveness between cells be required for cell movements to occur. Decreased integrin-mediated adhesion is also associated with cell migration on extracellular matrix molecules. For example, in smooth muscle cells, maximal migration occurs at intermediate attachment strengths (DiMilla *et al.*, 1993). It is possible, therefore, that overexpression of WT or DN XCdc42 disturbs the optimal

**FIG. 6.** XCdc42 functions downstream of the Wnt/$Ca^{2+}$ signaling pathway involving PKC activation. (A) (a) Uninjected animal caps treated with activin (10 ng/ml) showed extensive elongation. (b) Human PKC (hPKC)-$\alpha$ mRNA (0.5 ng per blastomere at the 4-cell stage) injection inhibited explant elongation. (c) Coinjection of DN XCdc42 mRNA (200 pg) with hPKC-$\alpha$ mRNA (2 ng) efficiently rescued the elongation of animal caps. (B) (a) Animal cap explants derived from uninjected control embryo elongated significantly in response to activin treatment. (b) Animal cap explants expressing XWnt-5a mRNA (800 pg) failed to elongate. (c) Rescue of XWnt-5a-inhibited explant elongation by coexpression of DN XCdc42 mRNA (300 pg). (d) Injection of mouse frizzled-3 (Mfz-3) mRNA (200 pg) inhibited activin-induced elongation. (e) Coexpression of DN XCdc42 mRNA (200 pg) reversed the inhibition of explant elongation caused by Mfz-3. (f) Control animal cap explants with no activin treatment remained rounded. (C) Quantitation of elongation of animal cap explants. RNAs expressed are indicated below graph. Control-1 and control-2 serve for hPKC-$\alpha$ and XWnt-5a and Mfz-3, respectively. n, total number of explants.

strength of cell adhesion required for cell movements to occur, leading to a common phenotype, the inhibition of cell movements, both in whole embryos and tissue explants. This hypothesis is corroborated by experiments in which the inhibition of activin-induced explant elongation caused by WT XCdc42 was optimally rescued by only intermediate doses of DN XCdc42, with higher doses doing so much less efficiently (our unpublished data).

Recently, it has been shown that the effect of *Xenopus* Wnt-11 and frizzled-7 on activin-induced explant elongation was efficiently reversed by a DN mutant of human Cdc42 (hCdc42) (Djiane *et al.*, 2000). Conversely, the effect of extra-Xfz7, a secreted form of the receptor, was rescued by a constitutively active mutant of hCdc42 (Djiane *et al.*, 2000). In our analysis, DN XCdc42 rescued Xwnt-11-inhibited elongation of animal cap explants, and a constitutively active XCdc42 recovered the inhibitory effect of a DN Xwnt-11 at relatively lower doses (data not shown). These results suggest that XCdc42 may be an effector of XWnt-11 and Xfz7 signaling. Although XWnt-11 and Xfz-7 could regulate cell polarity via dishevelled during convergent extension (Djiane *et al.*, 2000; Tada and Smith, 2000), it is tempting to speculate that in Xwnt-11 and Xfz7 signaling pathways, the inhibition of convergent extension caused by both gain- and loss-of-function (Du *et al.*, 1995; Tada and Smith, 2000; Djiane *et al.*, 2000) may be in part due to alteration in the ability of XCdc42 to maintain the optimal strength of cell adhesion required for cell movement and rearrangement.

Presumably, multiple components are required to coordinate the cell adhesion in tissues undergoing extensive morphogenetic movements such as convergent extension during gastrulation. Just as the enhancement of XCdc42 activity by its overexpression decreases the adhesiveness between neighboring cells (see Fig. 7), so XRnd1 acts to reduce cell adhesion in a GTP-dependent manner and possibly promotes cell rearrangements through loosening of cell contacts in the involuting mesoderm (Wünnenberg-Stapleton *et al.*, 1999). The loss of cell adhesion caused by XRnd1 could be rescued by only activated XRhoA that promotes cell adhesiveness (Wünnenberg-Stapleton *et al.*, 1999). In the future, it will be important to study the relationship between these GTPases and the molecular mechanism by which the relative activities of these molecules are adjusted in the regulation of cell adhesiveness in developing tissues.

Dsh's function in convergent extension movements in the *Xenopus* embryo is to form the polarized cell protrusions that are required for cell intercalation by controlling cell polarity (Wallingford *et al.*, 2000). In *Drosophila*, dishevelled signals to JNK via RhoA GTPase to regulate the cytoskeleton in the planar tissue polarity signaling pathway (Strutt *et al.*, 1997). Intriguingly, in vertebrates, dishevelled activates RhoA through a Dsh–RhoA complex formation mediated by Daam1, a scaffolding protein, and JNK activation by Dsh may be independent of RhoA (Habas *et al.*, 2001). Our analysis revealed that XCdc42 affects convergent extension independently of Dsh, as analyzed by an animal cap assay in which DN and constitutively active XCdc42 mutants could not rescue the inhibitory effects of truncated mutants (PDZ or DEP domain-deleted) and WT dishevelled on activin-induced explant elongation and vice versa (our unpublished data). Consistent with this, the DN mutant of Cdc42 could not inhibit Dsh-induced JNK activation in COS-7 cell (Lin *et al.*, 1999) and mouse dishevelled-2 activated RhoA and Rac but not Cdc42 in GST-RBD and GST-PBD binding assays (Habas *et al.*, 2001). XWnt-11 signaling regulates convergent extension movements via dishevelled (Tada and Smith, 2000) and induces Dsh-mediated RhoA activation (Habas *et al.*, 2001) in a *Drosophila* PCP-like pathway. In addition, Cdc42 may be an effector of the XWnt-11 signaling pathway (Djiane *et al.*, 2000; our unpublished data), while XCdc42 does not seem to act downstream or upstream of dishevelled. These results suggest that XWnt-11 may regulate Cdc42 and RhoA activities in a distinct manner during convergent extension, with Cdc42 in a novel pathway not involving dishevelled.

Recent experiments in *zebrafish* and *Xenopus* have shown that XWnt-5a and some vertebrate Frizzled receptor such as Rfz-2 and Mfz-3 can cause intracellular $Ca^{2+}$ release by activating the phosphatidylinositol pathway in a G-protein-dependent manner, leading to the translocation to the membrane, and activation, of PKC (Miller *et al.*, 1999; Kühl *et al.*, 2000a). We tested whether XCdc42 might participate in this Wnt/$Ca^{2+}$ signaling pathway involving PKC activation. In our experiment, DN XCdc42 efficiently rescued the inhibition of explant elongation caused by the overexpression of human PKC-$\alpha$ (Fig. 6A), suggesting that XCdc42 may function downstream of PKC-$\alpha$ in morphogenetic movements. This XCdc42 mutant also recovered the inhibitory effects of XWnt-5a and Mfz-3 on activin-induced elongation of animal cap explants (Fig. 6B). Taken together, these data indicate that XCdc42 may function downstream of a PKC-mediated Wnt/$Ca^{2+}$ signaling pathway in the regulation of convergent extension movements. XWnt-5a signal decreases $Ca^{2+}$-dependent cell adhesion, thereby affecting convergent extension movements in embryos (Torres *et al.*, 1996; Kühl *et al.*, 2000a). Our analyses have shown that DN XCdc42 reversed the effect of XWnt-5a overexpression to decrease the $Ca^{2+}$-dependent cell adhesion (Fig. 8), suggesting that XCdc42 may lie downstream of XWnt-5a in the modulation of cell adhesiveness.

Recent evidence reveals that XWnt-5a and XWnt-11 signal through a similar pathway. The effect of DN Wnt-11 to downregulate hyperphosphorylated dishevelled can be rescued by WT Wnt-11 and also Wnt-5a (Tada and Smith, 2000). The JNK pathway mediates the activities of Wnt-5a to regulate convergent extension movements in *Xenopus* (Yamanaka *et al.*, 2002). In addition, PKC, activated by the Wnt/$Ca^{2+}$ pathway, blocks the canonical Wnt/$\beta$-catenin pathway and phosphorylates dishevelled (Kühl *et al.*, 2001). In this regard, our result that XCdc42 functions downstream of PKC-mediated XWnt-5a and Dsh-independent XWnt-11 pathways suggests a possible Wnt-11 signaling mediated by PKC activation. Xfz-7 is also implicated in both the PCP pathway

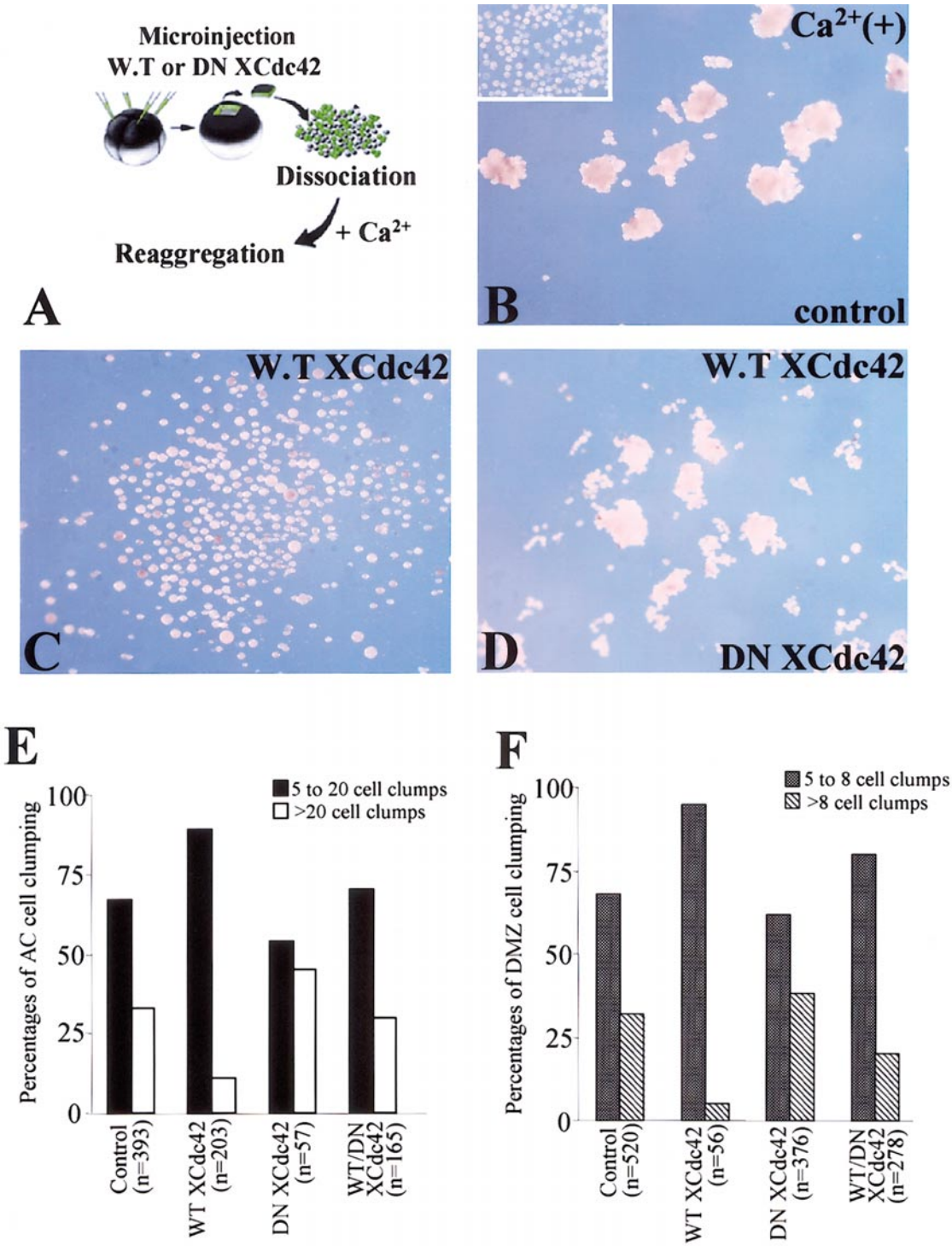


**FIG. 7.** Effects of XCdc42 on $Ca^{2+}$-dependent cell adhesion. (A) Experimental scheme of cell adhesion assay, which is described in more detail in Materials and Methods. Embryos were injected into animal pole (AC) or DMZ regions at the four-cell stage with WT XCdc42 mRNA (400–500 pg) or DN XCdc42 mRNA (0.5–2 ng). In a coinjection study, 400 (in DMZ cells) or 500 pg (in AC cells) of WT XCdc42 was injected with 400 or 800 pg of DN XCdc42, respectively. (B) Dissociated control explants reaggregate in a $Ca^{2+}$-dependent manner. In the absence of $Ca^{2+}$, reaggregation is inhibited (inset). (C) Overexpression of WT XCdc42 mRNA inhibits $Ca^{2+}$-dependent cell reaggregation, which can be rescued by coexpression of WT XCdc42 with DN XCdc42 mRNA (D). (E, F) Relative aggregation of animal cap and DMZ cells in $Ca^{2+}$-dependent cell adhesion assay, respectively. Constructs expressed are indicated below graph. The sizes of cell clumps are indicated in legend above graph. n, total number of cell clumps formed in five independent experiments.

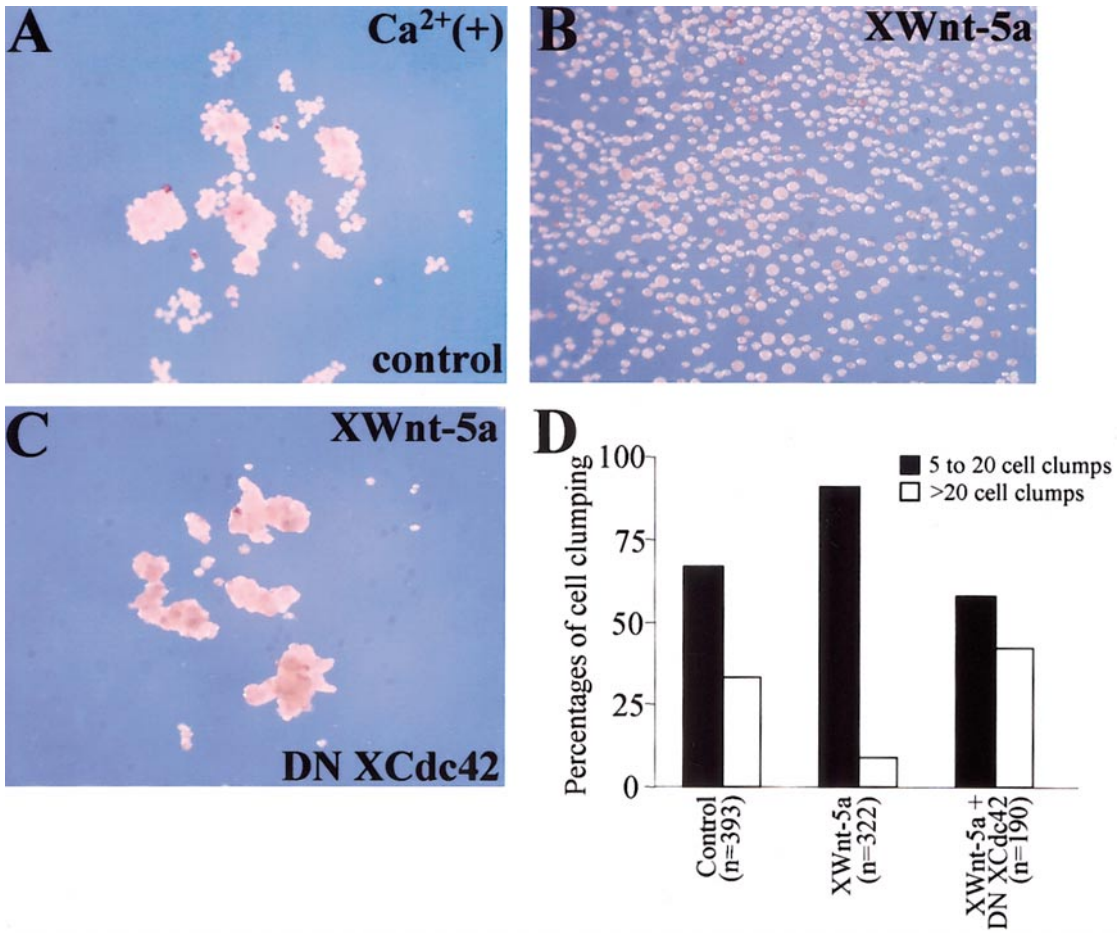


**FIG. 8.** XCdc42 acts downstream of XWnt-5a in a $Ca^{2+}$-dependent cell adhesion. (A) Cells from uninjected animal cap explants reaggregated into large clumps of cells in a $Ca^{2+}$-dependent manner. (B) Overexpression of XWnt-5a mRNA (2 ng at the 4-cell stage) inhibited $Ca^{2+}$-dependent cell reaggregation. (C) XWnt-5a-decreased $Ca^{2+}$-dependent cell adhesion was rescued by coexpressing DN XCdc42 mRNA (500 pg). (D) Relative cell aggregation in a $Ca^{2+}$-dependent cell adhesion assay. Constructs expressed are indicated below graph. The sizes of cell clumps are indicated in legend above graph. n, total number of cell clumps counted in five independent experiments.

involving Dsh-mediated RhoA activation (Djiane *et al.*, 2000; Habas *et al.*, 2001) and the PKC-dependent Wnt pathway (Medina *et al.*, 2000). It is possible that Wnt-11 and Wnt-5a, members of the same Wnt-5a class ligands, may function redundantly. There may, however, be a common pathway shared by both, downstream of which XCdc42 functions to regulate cadherin-mediated cell–cell adhesion (Kaibuchi *et al.*, 1999; Angst *et al.*, 2001) or cell polarity in morphogenetic movements. Identifying cytoplasmic factors, frizzled receptors, or coreceptors that contribute to the specificity of signal transduction triggered by each ligand is a priority for future research.

## ACKNOWLEDGMENTS

We thank Dr. Makoto Asashima for recombinant activin A, Dr. Michael King for the cDNA library, and Dr. Randall Moon for the generous gifts of plasmids. We are also grateful to B. H. Song for initial work in this study and other members of our laboratory for technical assistance and helpful discussion. This work was supported by a grant of the Korea Health 21 R&D Project, Ministry of Health & Welfare (01-PJ1-pg3–20700-0024), and Brain Korea 21 project.

## REFERENCES

Angst, B. D., Marcozzi, C., and Magee, A. I. (2001). The cadherin superfamily: Diversity in form and function. *J. Cell Sci.* **114,** 629–641.

Barrett, K., Leptin, M., and Settleman, J. (1997). The Rho GTPase and a putative RhoGEF mediate a signaling pathway for the cell shape changes in *Drosophila* gastrulation. *Cell* **91,** 905–915.

Bishop, A. L., and Hall, A. (2000). Rho GTPases. and their effector proteins. *Biochem. J.* **348,** 241–255.

Boutros, M., Paricio, N., Strutt, D. I., and Mlodzik, M. (1998). Dishevelled activates JNK and discriminates between JNK pathways in planar polarity and *wingless* signaling. *Cell* **94,** 109–118.

Bouwmeester, T., Kim, S. H., Sasai, Y., Lu, B., and De Robertis, E. M. (1996). Cerberus is a head-inducing secreted factor expressed in the anterior endoderm of Spemann's organizer. *Nature* **382,** 595–601.

Brieher, W. M., and Gumbiner, B. M. (1994). Regulation of C-Cadherin function during activin induced morphogenesis of *Xenopus* animal caps. *J. Cell Biol.* **126,** 519–527.

Cadigan, K. M., and Nusse, R. (1997). Wnt signaling: A common theme in animal development. *Genes Dev.* **11,** 3286–3305.

Dale, T. C. (1998). Signal transduction by the Wnt family of ligands. *Biochem. J.* **329,** 209–223.

DiMilla, P. A., Stone, J. A., Quinn, J. A., Albelda, S. M., and Lauffenburger, D. A. (1993). Maximal migration of human smooth muscle cells on fibronentin and type IV collagen occurs at an intermediate attachment strength. *J. Cell Biol.* **122,** 729–737.

Djiane, A., Riou, J. F., Umbhauer, M., Boucaut, J. C., and Shi, D. L. (2000). Role of *frizzled 7* in the regulation of convergent extension movements during gastrulation in *Xenopus laevis*. *Development* **127,** 3091–3100.

Drechsel, D. N., Hyman, A. A., Hall, A., and Glotzer, M. (1996). A requirement for Rho and Cdc42 during cytokinesis in *Xenopus* embryos. *Curr. Biol.* **7,** 12–23.

Du, S. J., Purcell, S. M., Christian, J. L., McGrew, L. L., and Moon, R. T. (1995). Identification of distinct classes and functional domains of Wnts through expression of wild-type and chimeric proteins in *Xenopus* embryos. *Mol. Cell. Biol.* **15,** 2625–2634.

Erickson, J. W., and Cerione, R. A. (2001). Multiple roles for Cdc42 in cell regulation. *Curr. Opin. Cell Biol.* **13,** 153–157.

Gawantka, V., Delius, H., Hirschfeld, K., Blumenstock, C., and Niehrs, C. (1995). Antagonizing the Spemann organizer: Role of the homeobox gene *Xvent-1*. *EMBO J.* **14,** 6268–6279.

Godsave, S. F., Isaac, H., and Slack, J. M. W. (1988). Mesoderm inducing factors: A small class of molecules. *Development* **102,** 555–566.

Habas, R., Kato, Y., and He, X. (2001). Wnt/frizzled activation of Rho regulates vertebrate gastrulation and requires a novel formin homology protein Daam1. *Cell* **107,** 843–854.

Harland, R. M. (1991). In situ hybridization: An improved whole-mount method for *Xenopus* embryos. *Methods Cell Biol.* **36,** 685–695.

Heisenberg, C. P., Tada, M., Rauch, G. J., Saúde, L., Concha, M., Geisler, R., Stemple, D. L., Smith, J. C., and Wilson, S. W. (2000). Silberblick/Wnt11 mediates convergent extension movements during zebrafish gastrulation. *Nature* **405,** 76–81.

Henry, G. L., Brivanlou, I. H., Kessler, D. S., Hemmati-Brivanlou, A., and Melton, D. A. (1996). TGF-$\beta$ signals and a prepattern in *Xenopus laevis* endodermal development. *Development* **122,** 1007–1015.

Huttenlocher, A., Sandborg, R. R., and Horwitz, A. F. (1995). Adhesion in cell migration. *Curr. Opin. Cell Biol.* **7,** 697–706.

Kaibuchi, K., Kuroda, S., Fukata, M., and Nakagawa, M. (1999). Regulation of cadherin-mediated cell–cell adhesion by the Rho family GTPases. *Curr. Opin. Cell Biol.* **11,** 591–596.

Keller, R. (1991). Early embryonic development of *Xenopus laevis*. *Methods Cell Biol.* **36,** 61–113.

Keller, R., Shih, J., and Domingo, C. (1992). The patterning and functioning of protrusive activity during convergence and extension of the *Xenopus* organizer. *Dev. Suppl.,* 81–91.

Kengaku, M., and Okamoto, H. (1995). bFGF as a possible morphogen for the anteroposterior axis of the central nervous system in *Xenopus*. *Development* **121,** 3121–3130.

Kim, M. J., and Han, J. K. (1999). The involvement of cAMP signaling pathway in axis specification in *Xenopus* embryos. *Mech. Dev.* **89,** 55–64.

Krasnow, R. E., and Adler, P. N. (1994). A single frizzled protein has a dual function in tissue polarity. *Development* **120,** 1883–1893.

Kühl, M., Sheldahl, L. C., Park, M., Miller, J. R., and Moon, R. T. (2000a). The Wnt/$Ca^{2+}$ pathway a new vertebrate Wnt signaling pathway takes shape. *Trends Genet.* **16,** 279–283.

Kühl, M., Sheldahl, L. C., Malbon, C. C., and Moon, R. T. (2000b). $Ca^{2+}$/Calmodulin-dependent protein kinase II is stimulated by Wnt and Frizzled homologs and promotes ventral cell fates in *Xenopus*. *J. Biol. Chem.* **275,** 12701–12711.

Kühl, M., Geis, K., Sheldahl, L. C., Pukrop, T., Moon, R. T., and Wedlich, D. (2001). Antagonistic regulation of convergent extension movements in *Xenopus* by Wnt/$\beta$-catenin and Wnt/$Ca^{2+}$ signaling. *Mech. Dev.* **106,** 61–76.

Lamb, T. M., Knecht, A. K., Smith, W. C., Stachel, S. E., Economides, A. N., Stahl, N., Yancopolous, G. D., and Harland, R. M. (1993). Neural induction by the secreted polypeptide noggin. *Science* **262,** 713–718.

Lemaire, P., and Gurdon, J. B. (1994). A role for cytoplasmic determinants in mesoderm patterning: Cell-autonomous activation of *goosecoid* and *Xwnt-8* along the dorsoventral axis of early *Xenopus* embryos. *Development* **120,** 1191–1199.

Lemaire, P., Garrett, N., and Gurdon, J. B. (1995). Expression cloning of *Siamois*, a *Xenopus* homeobox gene expressed in dorsal–vegetal cells of blastulae and able to induce a complete secondary axis. *Cell* **81,** 85–94.

Lin, L., Yuan, H., Xie, W., Mao, J., Caruso, A. M., McMahon, A., Sussman, D. J., and Wu, D. (1999). Dishevelled proteins lead to two signaling pathways. *J. Biol. Chem.* **274,** 129–134.

Medina, A., Reintsch, W., and Steinbeisser, H. (2000). *Xenopus frizzled7* can act in canonical and non-canonical Wnt signaling pathways: Implications on early patterning and morphogenesis. *Mech. Dev.* **92,** 227–237.

Miller, J. R., Hocking, A. M., Brown, J. D., and Moon, R. T. (1999). Mechanism and function of signal transduction by the Wnt/$\beta$-catenin and Wnt/$Ca^{2+}$ pathways. *Oncogene* **18,** 7860–7872.

Moon, R. T., and Kimelman, D. (1998). From cortical rotation to organizer gene expression: Toward a molecular explanation of axis specification in *Xenopus*. *BioEssays* **20,** 536–545.

Moriguchi, T., Kawachi, K., Kamakura, S., Masuyama, N., Yamanaka, H., Matsumoto, K., Kikuchi, A., and Nishida, E. (1999). Distinct domains of mouse dishevelled are responsible for the c-Jun N-terminal kinase/stress-activated protein kinase activation and the axis formation in vertebrates. *J. Biol. Chem.* **274,** 30957–30962.

Nieuwkoop, P. D., and Faber, J. (1967). "Normal Table of *Xenopus laevis (Daudin)*," North Holland, Amsterdam.

Piccolo, S., Sasai, Y., Lu, B., and De Robertis, E. M. (1996). Dorsoventral patterning in *Xenopus*: Inhibition of ventral signals by direct binding of chordin to BMP-4. *Cell* **86,** 589–598.

Schmitz, A. A. P., Govek, E. E., Böttner, B., and Aelst, L. V. (2000). Rho GTPases. Signaling, migration, and invasion. *Exp. Cell Res.* **261,** 1–12.

Sheldahl, L. C., Park, M., Malbon, C. C., and Moon, R. T. (1999). Protein kinase C is differentially stimulated by Wnt and Frizzled homologs in a G-protein-dependent manner. *Curr. Biol.* **9,** 695–698.

Slusarski, D. C., Yang-Snyder, J., Busa, W. B., and Moon, R. T. (1997a). Modulation of embryonic intracellular $Ca^{2+}$ signaling by *Wnt-5A*. *Dev. Biol.* **182,** 114–120.

Slusarski, D. C., Corces, V. G., and Moon, R. T. (1997b). Interaction of Wnt and a Frizzled homologue triggers G-protein-linked phosphatidyl inositol signaling. *Nature* **390,** 410–413.

Smith, J. C., Price, B. M. J., Green, J. B. A., Weigel, D., and Herrmann, B. G. (1991). Expression of a *Xenopus* homolog of *Brachyury (T)* is an immediate-early response to mesoderm induction. *Cell* **67,** 79–87.

Smith, W. C., McKendry, R., Ribisi, S., Jr., and Harland, R. M. (1995). A *nodal-related gene* defines a physical and functional domain within the Spemann organizer. *Cell* **82,** 37–46.

Strutt, D. I., Weber, U., and Mlodzik, M. (1997). The role of RhoA in tissue polarity and Frizzled signaling. *Nature* **387,** 292–295.

Symes, K., and Smith, J. C. (1987). Gastrulation movements provide an early marker of mesoderm induction in *Xenopus laevis*. *Development* **101,** 339–349.

Tada, M., and Smith, J. C. (2000). *Xwnt11* is a target of *Xenopus* Brachyury: Regulation of gastrulation movements via Dishevelled, but not through the canonical Wnt pathway. *Development* **127,** 2227–2238.

Torres, M. A., Yang-Snyder, J. A., Purcell, S. M., DeMarais, A. A., McGrew, L. L., and Moon, R. T. (1996). Activities of the *Wnt-1* class of secreted signaling factors are antagonized by the *Wnt*-5A class and by a dominant negative cadherin in early *Xenopus* development. *J. Cell Biol.* **133,** 1123–1137.

Wallingford, J. B., Rowning, B. A., Vogeli, K. M., Rothbächer, U., Fraser, S. E., and Harland, R. M. (2000). Dishevelled controls cell polarity during *Xenopus* gastrulation. *Nature* **405,** 81–85.

Wallingford, J. B., and Harland,R. M. (2001). *Xenopus* Dishevelled signaling regulates both neural and mesodermal convergent extension: Parallel forces elongating the body axis. *Development* **128,** 2581–2592.

Wong, G. T., Gavin, B. J., and McMahon, A. P. (1994). Differential transformation of mammary epithelial cells by Wnt genes. *Mol. Cell. Biol.* **14,** 6278–6286.

Wünnenberg-Stapleton, K., Blitz, I. L., Hashimoto, C., and Cho, K. W. Y. (1999). Involvement of the small GTPases XRhoA and XRnd1 in cell adhesion and head formation in early *Xenopus* development. *Development* **126,** 5339–5351.

Yamanaka, H., Moriguchi, T., Masuyama, N., Kusakabe, M., Hanafusa, H., Takada, R., Takada, S., and Nishida, E. (2002). JNK functions in the non-canonical Wnt pathway to regulate convergent extension movements in vertebrates. *EMBO Rep.* **3,** 69–75.

Received for publication December 11, 2001
Revised January 17, 2002
Accepted January 17, 2002
Published online March 11, 2002